DYNAMIC ANALYSIS OF GENEVA MECHANISMS WITH SPECIAL CONSIDERATION TO REVERSES OF PINS

By

E. FILEMON

Department for Technical Mechanics, Polytechnical University, Budapest

Presented by Prof. DR. G. KOZMANN

(Received August 22, 1960)

Introduction

Geneva mechanisms producing intermittent motion have widely spread because of their simple construction and long duration of life. However, the latter may be attained only in case they are impeccably designed and correctly operated. Inadequate design and bad handling will cause their untimely wear and quick breakdown. This is why their dynamic analysis has become

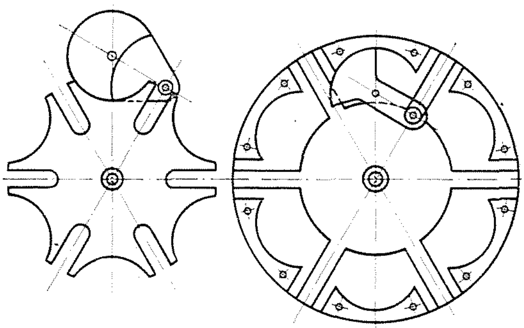

Fig. 1

essential. An approach through mathematical methods of the problem facilitates the reaching of general conclusions, therefore, it is preferable to graphical methods. As regards construction, Geneva motions may be of external or internal drive type (Fig. 1). As a Geneva mechanism may be traced back to a swing link, it is evident that external drive is at a disadvantage as regards both kinematic and dynamic conditions. (The quick motion of link mechanism.) The present paper covers the investigation of the external drive Geneva mechanisms and pays special attention to the determination of the number and location of pin reverses (the passing of the driving pin from one side of the slot to the other) ; and following this, examines the determination of the moment important in designing.

The conditions of the dynamic analysis

Fig. 2 shows a four-slot construction ($n = 4$) and the symbols used. The number of slots ou denoted by n and the distance between the axes is r_1. Since the mechanism under examination is univariant, the moment M_2 reduced to the driving member (2) may be determined. The drive torque has to keep balance with this reduced moment. Thus, provided the variation of reduced moment M_2 is known, the power necessary for the overcoming of the opposition can be worked out. The moments may be reduced on the basis of equal performances

$$N_2 = \Sigma N_i$$

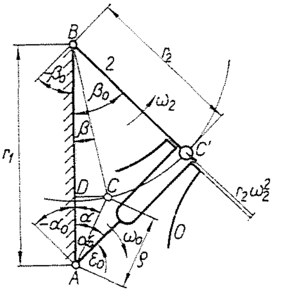

Fig. 2

or, neglecting friction,

$$M_2\,\omega_2 = M_0\,\omega_0$$

where

$$M_0 = M_e + \Theta_0\,\varepsilon_0$$

The symbols used in the equation are :

M_2 = torque acting on the driving shaft of the Geneva mechanism
ω_2 = angular velocity of the driving member
M_e = anti-torque moment (*e. g.* useful opposition)
Θ_0 = the moment of inertia of the driven members connected to the axle of the Geneva
ε_0 = angular acceleration of the follower (maltese cross)
ω_0 = angular velocity of follower (maltese cross).

Taking the efficiency of the Geneva mechanism into consideration, we may write

$$M_2 = \frac{\omega_0}{\omega_2}\,\frac{1}{\eta}\,[M_e + \Theta_0\,\varepsilon_0] \tag{1}$$

The variation of M_2 may be determined only when the variation of the kinematic characteristics are known.

Kinematic analysis

From triangle ABC, Fig. 2 follows

$$\overline{AC} = \varrho = \sqrt{r_1^2 + r_2^2 - 2r_1 r_2 \cos\beta}$$

since $r_2 = r_1 \sin \alpha_0$ (from rectangular triangle ABC′), and $\alpha_0 = \frac{\pi}{n}$; in case of a specified number of slots

$$\sin \alpha_0 = \frac{r_2}{r_1} = c = \text{constant}$$

thus

$$\varrho = r_1 \sqrt{1 + c^2 - 2c\cos\beta}\,.$$

As follows from the figure

$$\overline{CD} = r_2 \sin_\beta = \varrho \sin \alpha,$$

hence

$$\sin \alpha = \frac{c \sin\beta}{\sqrt{1 + c^2 - 2c\cos\beta}}\,.$$

The angular velocity

$$\omega_0 = \frac{d\alpha}{dt}$$

because of

$$\alpha = f(\beta);\ \omega_0 = \frac{d\alpha}{d\beta}\frac{d\beta}{dt}.$$

Substitute

$$\frac{d\beta}{dt} = \omega_2$$

then

$$\omega_0 = \omega_2 \frac{d\alpha}{d\beta}\,.$$

Introducing the notation $i_\omega = \frac{\omega_0}{\omega_2}$; then in case $\omega_2 =$ constant, i_ω varies in proportion to the variation of ω_0.

$$i_\omega = \frac{d\alpha}{d\beta} = \frac{c(\cos\beta - c)}{1 + c^2 - 2c\cos\beta}\,. \tag{2}$$

Chosing the number of slots at will; i_ω varies as shown in Fig. 3. It can be seen that when $\beta = 0°$ then $i_\omega = i_{\omega\,\max}$. By substituting:

$$i_{\omega\,\max} = \frac{c}{1-c}\,.$$

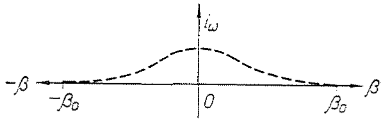

Fig. 3

Fig. 4 shows i_ω diagrams for various slot numbers. In Table I $i_{\omega\max}$ values are also listed apart. The course of the curves has undergone a change as compared to those in Fig. 3 because of the axis i_ω constructed in logarithmic scale. The curves shape their courses to the perpendicular of angles β_0

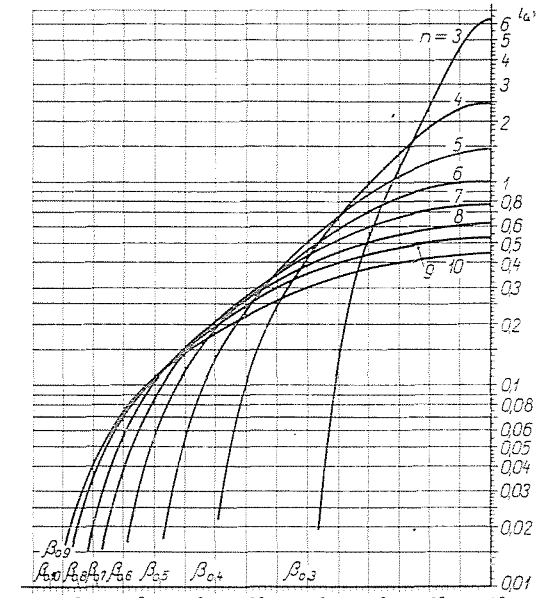

Fig. 4

asymptotically. The magnitudes of angles β_0 are indicated in the diagrams. The curves i_ω are symmetrical to the i_ω axis, therefore, only the values of the function between the limits $-\beta_0 < \beta < 0$ have been considered in Figure 4. The angular acceleration

$$\varepsilon_0 = \frac{d\omega_0}{dt} = \omega_2^2\,\frac{d^2 a}{d\beta^2}$$

may be introduced also here. With the notation

$$i_\varepsilon = \frac{\varepsilon_0}{\omega_2^2}$$

we may write

$$i_\varepsilon = \frac{d^2 a}{d\beta^2} = \frac{-c(1-c^2)\sin\beta}{(1+c^2-2c\cos\beta)^2}. \tag{3}$$

The curve $i\varepsilon$ connected to a specified number n is shown in Fig. 5. At the start $\beta = -\beta_0$; as seen in Fig. 2, the acceleration $r_2\,\omega_2^2$ coming from the rotation of member (2) is tangential as regards the cross, thus

$$(\varepsilon_0)_{\beta 0} = \frac{r_2}{r_0}\,\omega_2^2 .$$

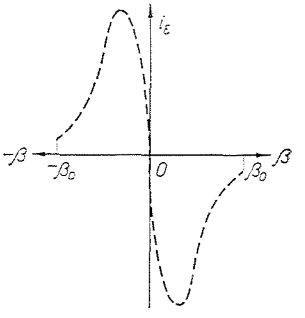

Fig. 5

In this position

$$(i_\varepsilon)_{\beta 0} = \operatorname{tg} a_0 . \tag{4}$$

By further increasing β, through the portion $-\beta_0 < \beta < 0$ i_ε is positive (acceleration).
It reaches maximum at

$$\frac{d^3 a}{d\beta^3} = 0 .$$

$$\frac{d^3 a}{d\beta^3} = -c(1-c^2)\,\frac{2c\cos^2\beta + (1-c^2)\cos\beta - 4c}{(1+c^2-2c\cos\beta)^3} = 0$$

Hence

$$\cos\beta_{\max} = -\frac{1+c^2}{4c} \pm \sqrt{\left[\frac{1+c^2}{4c}\right]^2 + 2} .$$

As the value of the radical is greater than unity, working only with the positive sign

$$\beta_{\max} = \operatorname{arc\,cos}\left[-\frac{1+c^2}{4c} + \sqrt{\left[\frac{1+c^2}{4c}\right]^2 + 2}\,\right]. \tag{5}$$

The values $\beta_{\max}$ are listed in Table I.

Table I

n	3	4	5	6	7	8	9	10
$i_{\omega \max}$	6.462	2.415	1.426	1.000	0.766	0.620	0.520	0.447
$\beta_{\max}$	4°46′	11°24′	17°34′	22°54′	27°33′	31°38′	35°16′	38°30′
$i_{\varepsilon s}$	1.732	1.—	0.7265	0.5774	0.4816	0.4142	0.3640	0.3249
$i_{\varepsilon \max}$	31.44	5.409	2.299	1.350	0.9284	0.6998	0.5591	0.4648
F_{12}	0.0318	0.1848	0.4349	0.4707	1.077	1.428	1.788	2.151
F_{23}	0.5774	1.—	1.3763	1.732	2.0765	2.4144	2.7485	3.0711

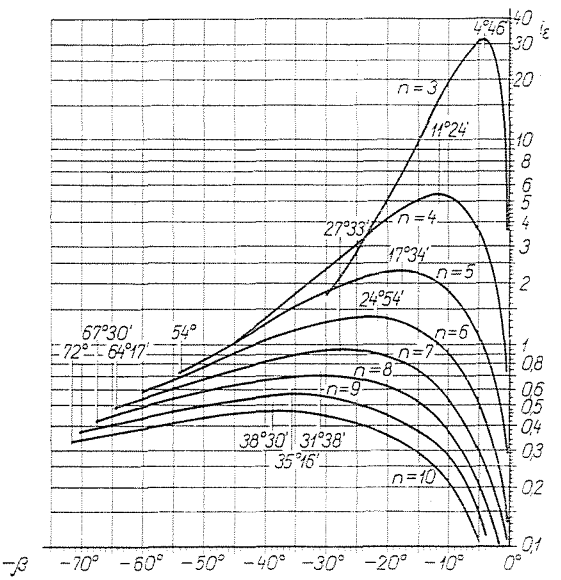

Fig. 6

Thus

$$i_{\varepsilon \max} = \frac{-c\,(1-c^2)\sin \beta_{\max}}{(1+c^2-2c\cos \beta_{\max})^2}\,.$$

Table I also contains the values $i_{\varepsilon \text{start}} = i_{\varepsilon s}$ and $i_{\varepsilon \max}$. Through the portion $0°$ to $-\beta_0$ of the function i_ε the ordinates have the same magnitudes but with negative signs (according to Fig. 5). This corresponds to a decelerating motion.

Assuming various slot numbers n we obtain the set of curves in Fig. 6. The alteration in the shape of the curves is again due to the logaritmic scale used for the axis i_ε. Similarly to the set of curves i_ε will also here do with the variations of angle β between the limits $-\beta_0 < \beta < 0$.

By using diagrams No. 4 and 6 we find $\omega_0 = i_\omega\,\omega_2$, and $\varepsilon_0 = i_\varepsilon\,\omega_2^2$.

Dynamic analysis

After this excursus necessary for further work let us turn to dynamic analysis. We may write

$$M_2 = [M_\varepsilon + \Theta_0 \, i_\varepsilon \, \omega_2^2] \, i_\omega \, \frac{1}{\eta} \, .$$

Introducing the notation

$$M_2 = \frac{\Theta_0 \, \omega_2^2}{M_\varepsilon}$$

we obtain

$$M_2 = M_\varepsilon \, [1 + F i_\varepsilon] \, i_\omega \, \frac{1}{\eta}$$

or

$$M_2 = \frac{M_\varepsilon}{\eta} \, [i_\omega + F i_\varepsilon \, i_\omega]. \tag{6}$$

By neglecting the variation of M_ε, the term $\frac{M_\varepsilon}{\eta}$ becomes constant and the variation of moment M_2 is a function of the term in brackets.

Fig. 7 shows the curves i_ω, i_ε and $i_\omega \, i_\varepsilon$ for $n = 4$. Curve M_2 represents the summation of two curves, namely $i_\omega + F \, i_\varepsilon \, i_\omega$. In Fig. 7 $F = 1$, moment M_2 is composed of positive and negative portions. Between $-\beta_0^\circ$ and 0° the moment is positive independently from the value of F, yet between 0° and β_0° the alteration of constant F may produce three variants (Fig. 8).

1. It may be assumed that with a certain value of F the intersect of the negative branch of the product curve $F \, i_\omega \, i_\varepsilon$ will be smaller in absolute value at any angle than i_ω belonging to the same angle β. Then M_2 changes as demonstrated in Fig. 8/*a* and continues to be positive throughout the whole cycle of motion. This means that the pin engages only one side of the slot of the cross and does not reverse in the whole course of the motion.

2. When increasing F the expected situation may be that the absolute values of the intersects $F \, i_\omega \, i_\varepsilon$ exceed the i_ω intersects only along a certain portion. Curve M_2 has a negative branch at this part and the moment M_2 is positive, changes into negative and becomes positive again, passing twice through zero in addition to the positions of start and stop in the same cycle of motion (Fig. 8/b). In the course of the motion, at a certain angle, β the driwing pin leaves the side of the slot it had engaged before and catches the opposite side (reverses). Before the motion is completed, the pin once more reverses. The double reversing renders the operation noisy, produces undesirable vibration, strains the slot and may result in breaking the pin. Therefore, this occurrence must be warded of by circumspect designing.

3. By further increasing the constant F, at some angle β the absolute value of the product $F\, i_\omega\, i_\varepsilon$ reaches the value of i_ω and keeps above it to the end. This same is demonstrated in Fig. 7 with $F = 1$. As F depends on the anti-torque moment M_e, on the angular velocity of the driving shaft, ω_2^2 and on the moment of inertia of the driven members (follower and attached parts), Θ_0, a careful selection and combination of the designing and operating conditions permits to obtain a positive torque throughout the whole motion. For a quick survey of the conditions of pin reversings the values of F corresponding to transitions among the three cases described above may be used.

The critical range of F may be determined by equating M_2 to 0.

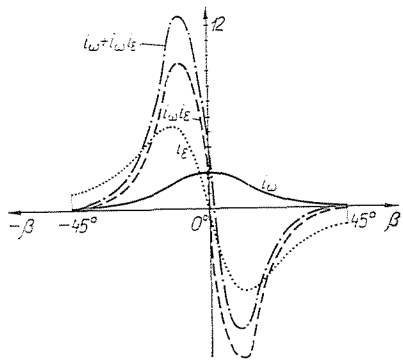

Fig. 7

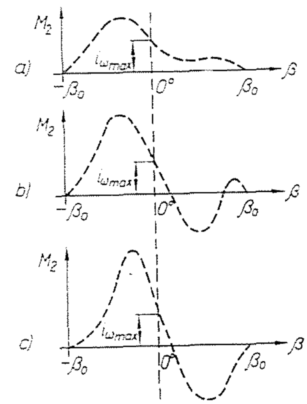

Fig. 8

$$M_2 = \frac{M_e}{\eta}\, i_\omega [1 + F i_\varepsilon]$$

$$M_2 = 0 \text{ when}$$

$$\frac{M_2}{\eta}\, i_\omega = 0; \quad \text{or} \quad 1 + F i_\omega = 0$$

$$\frac{M_e}{\eta}\, i_\omega = 0 \quad \text{when} \quad i_\omega = 0; \quad \text{this corresponds}$$

to the points $\beta = -\beta_0$ and $\beta = \beta_0$, that is to say, the moment equals zero at the instants of the beginning and ending of the motion.

From the condition

$$1 + F i_\varepsilon = 0$$

follows

$$F = -\frac{1}{i_\varepsilon} = \frac{(1 + c^2 - 2c\cos\beta)^2}{c\,(1 - c^2 \sin\beta)} . \tag{7}$$

The negative sign denotes a positive value of F since i_ε is negative on the portion $0 < \beta < \beta_0$.

Fig. 9 shows the variation of F, as results from Equ. (7) for the case the number of slots $n = 8$. The course of this diagram confirms the deductions inferred from Fig. 7 and 8. The points of intersection of the lines $F =$ constant with the curve marking out the angles β connected to the places $M_2 = 0$. It is to be seen that in zone 1 there is no intersection at all (M_2 does not equal zero at any part, Fig. 8/a); in zone 2 there are two intersections ($M_2 = 0$ twice, Fig. 8/b); in zone 3 there is one intersection ($M_2 = 0$ once,

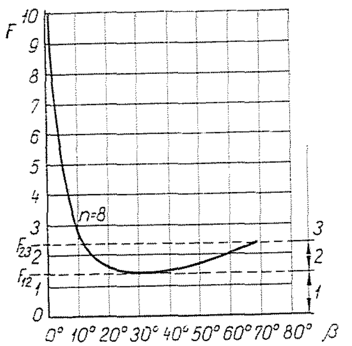

Fig. 9

Fig. 8/c). The critical range falls in zone 2, limited by the values F_{12} and F_{23}.

Assuming various slot numbers and determining F values result in the set of curves shown in Fig. 10.

On all the curves represented in the figure $F_{12} = F_{\min}$, therefore the extreme values of the curves $F = f(\beta)$ must be examined.

$$\frac{dF}{d\beta} = 0 = 4c \sin^2 \beta \ (1 - 2c \cos \beta + c^2) - (1 - 2c \cos \beta + c^2)^2 \cos \beta .$$

Since $(1 - 2c \cos \beta + c^2) \neq 0$. Divide by this throughout and transpose the equation for $\cos \beta$:

$$\cos \beta = - \frac{1 - c^2}{4c} + \sqrt{\left[\frac{1 - c^2}{4c}\right]^2 + 2} \ .$$

The result is in agreement with the term $\cos \beta_{\max}$ connected to the values $i_{\varepsilon \max}$. Transposing into Equ. (7)

$$F_{12} = - \frac{1}{i_{\varepsilon\max}} \qquad (8)$$

Considering Equ. (7) this result was to be expected.

The line $F =$ constant is tangent to the curve, the increase of F results in two points of intersection. Therefore, it is apparent that the condition of the determination of F_{23} is that one of the two points of intersection disap-

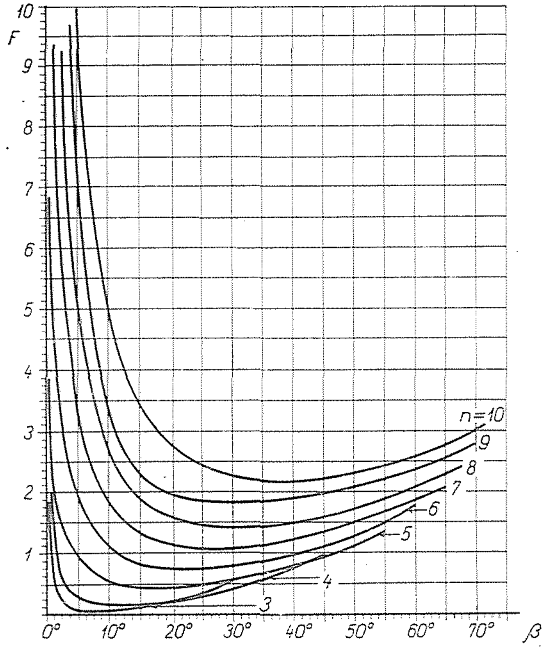

Fig. 10

pears, *i. e.* coincides with angle β_0, at which position the driving pin leaves the cross.

Transposition of $\beta = \beta_0$ into Equ. (7) gives

$$F_{23} = -\frac{1}{(i_\varepsilon)_{\beta_0}} = -\frac{1}{i_{\varepsilon s}}.$$

The term $i_{\varepsilon s}$ is defined by Equ. (4), thus

$$F_{23} = -\frac{1}{\operatorname{tg} a_0} = \operatorname{tg} \beta_0. \tag{9}$$

The values worked out of F_{12} and F_{23} are given in Table I and represented in Fig. 11.

According to the above, the conditions of pin reversings in Geneva mechanisms may be determined and controlled.

The next task is to work out the power demand

$$N_2 = M_{2av}\omega_2.$$

The torque required to rotate the crankshaft has to overcome the opposition originating on the shaft of the cross, plus the resistance produced by the accelerations. As long as the cross picks up speed (in the first half of the revolution) the moment of inertia adds to the resistance. The value of the average moment $(M_{2\,av})$ has to be determined for the interval $-\beta_0 < \beta < 0$.

$$M_{2av} = \frac{1}{\beta_0} \frac{M_e}{\eta} \int_{-\beta_0}^{0} (i_\omega + F i_\omega i_\varepsilon)\, d\beta .$$

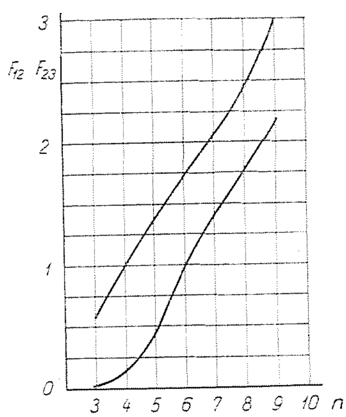

Fig. 11

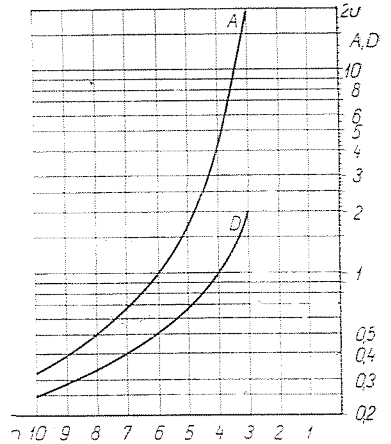

Fig. 12

In conclusion the following relationship is obtained

$$M_{2av} = D M_e \frac{1}{\eta} (1 + FA) \tag{10}$$

where

$$D = \frac{2}{n-2} \quad \text{and} \quad A = \frac{n}{2\pi} \left(\frac{c}{1-c} \right)^2 .$$

In Fig. 12 the values D and A are given as functions of n.

In order to facilitate the determination of M_{2av} the nomogram in Fig. 13 was constructed and its use explained in Fig. 14. In case we want to improve the accuracy of reading, the M_2 values may be multiplied by any chosen power of 10. (It should be kept in mind that this operation causes the result to change by a corresponding order of magnitude.)

In case a Geneva mechanism is to have its own driving motor, at the selection of the latter the existence of a maximum moment in the first half revolution shall also be taken into consideration. M_{2max} is to be determined and the ratio of the maximum and average moments found. If this ratio is s ma

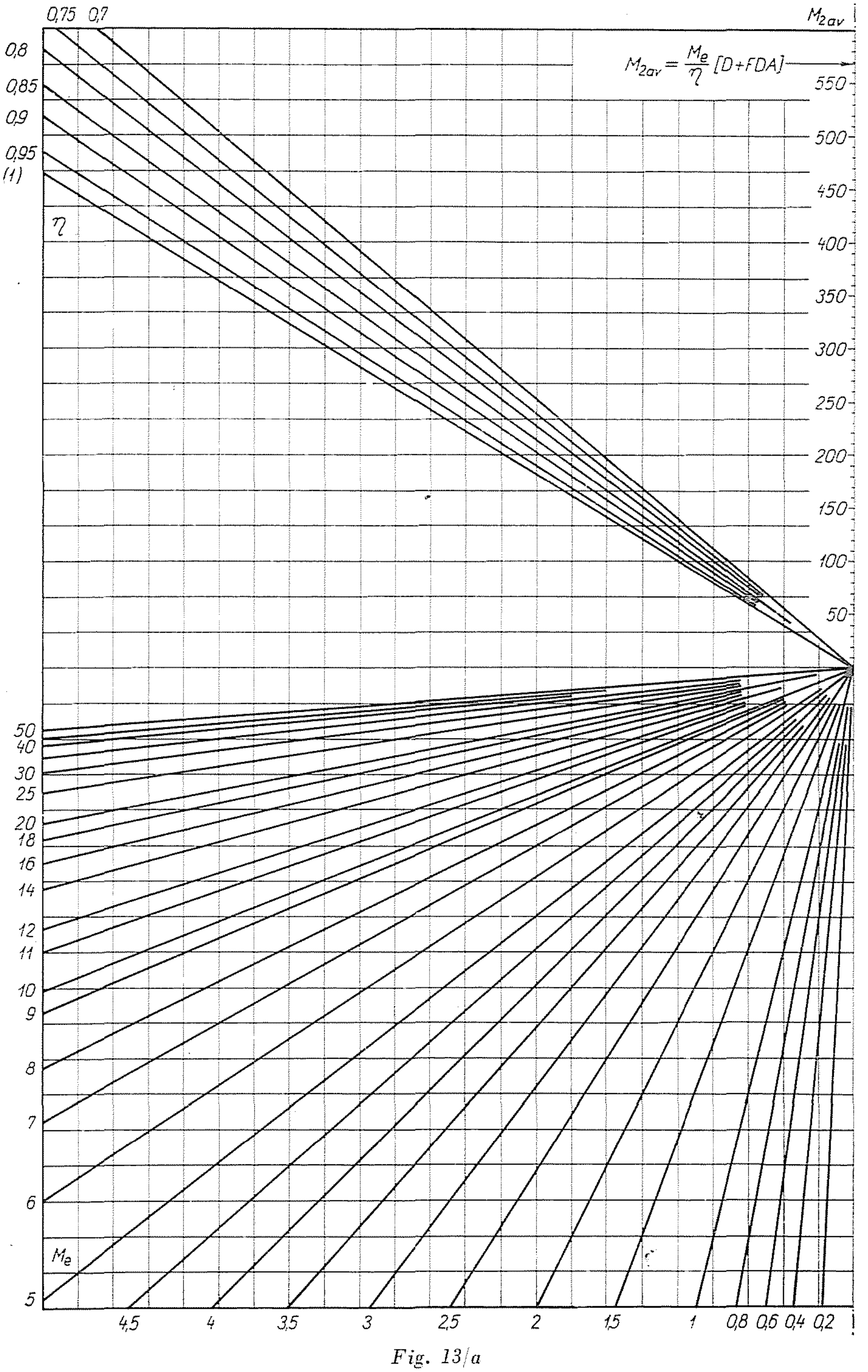
0,75
0,7
M_{2av}
0,8
0,85
0,9
0,95
(1)
η
$M_{2av} = \frac{M_e}{\eta} [D+FDA]$
550
500
450
400
350
300
250
200
150
100
50
50
40
30
25
20
18
16
14
12
11
10
9
8
7
6
M_e
5
4,5
4
3,5
3
2,5
2
1,5
1
0,8
0,6
0,4
0,2

Fig. 13/a

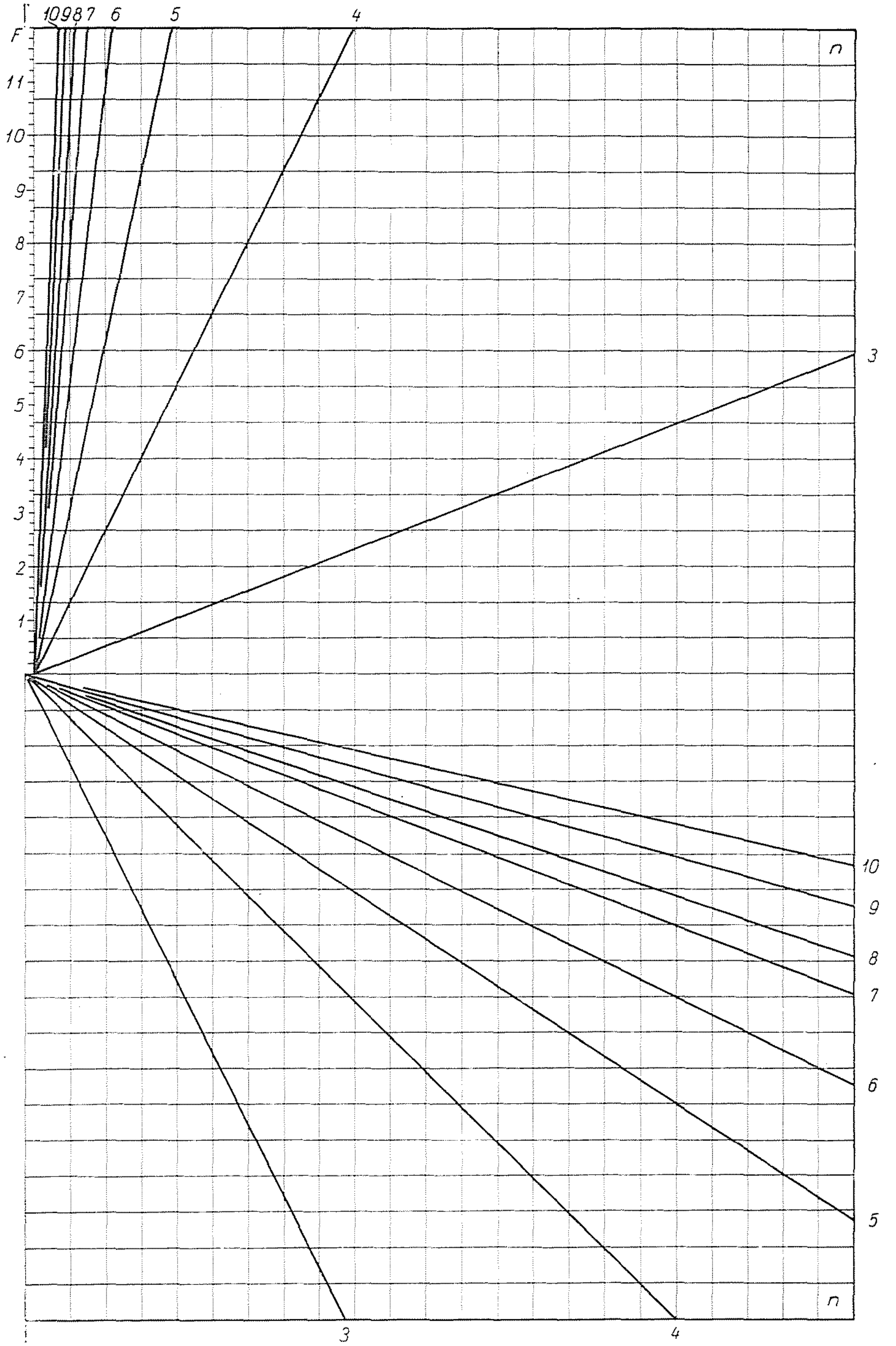

Fig. 13/b

(to about $n > 6$) the excess load factor of a motor selected on the basis of M_{2av} is enough tu guarantee that the motor will stand the expected peak power demand without danger. If this ratio is still large (from about $n < 6$)

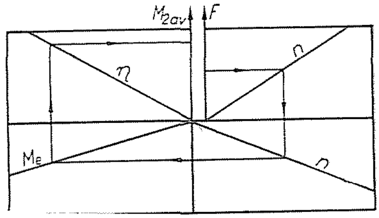

Fig. 14

the motor cannot be selected on the basis of M_{2av} but $M_{2\max}$ should be considered instead, and values reaching multiples of M_{2av} might be required.

Let us pass on to the determination of $M_{2\max}$.

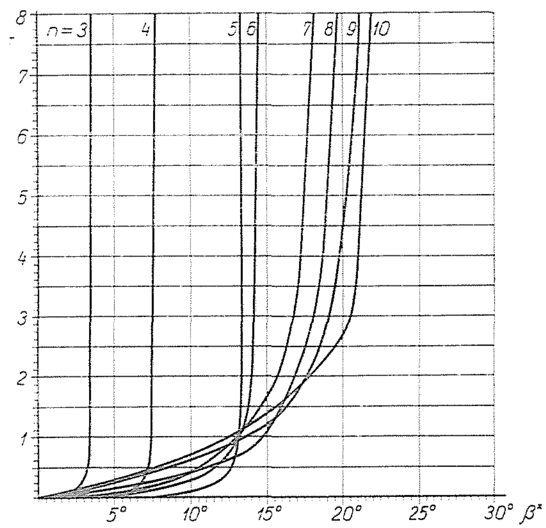

Fig. 15

As is seen in Fig. 8, out of the limit values of M_2 it is the positive maximum in the first part of the rotation ($-\beta_0 < \beta < 0$) that gives the absolute maximum. The investigation of the limit values will be restricted to this part.

M_2 reaches limit value at the point $\frac{dM_2}{d\beta} = 0$.

$$\frac{dM_2}{d\beta} = 0 = -\frac{c(1-c^2)\sin\beta}{(1-2c\cos\beta+c^2)^2} - Fc^2(1-c^2)\cdot$$

$$\cdot\frac{2c\cos^3\beta + 2(1-c^2)\cos^2\beta - (5c+c^3)\cos\beta + 5c^2 - 1}{(1-2c\cos\beta+c^2)^4}.$$

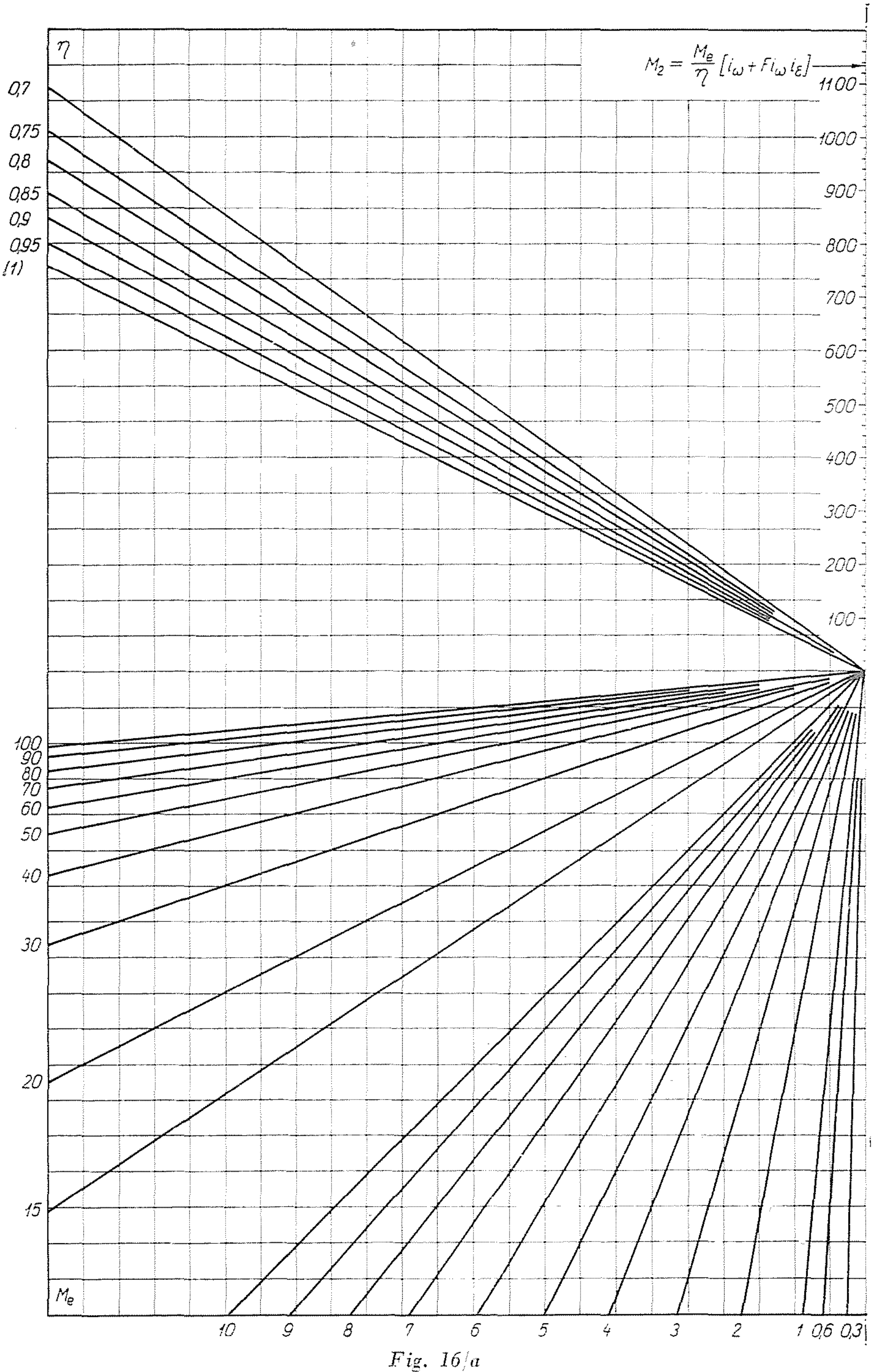
η
0,7
0,75
0,8
0,85
0,9
0,95
(1)
$M_2 = \frac{M_e}{\eta}[i_\omega + Fi_\omega i_\varepsilon]$
1100
1000
900
800
700
600
500
400
300
200
100
100
90
80
70
60
50
40
30
20
15
M_e
10
9
8
7
6
5
4
3
2
1
0,6
0,3

Fig. 16/a

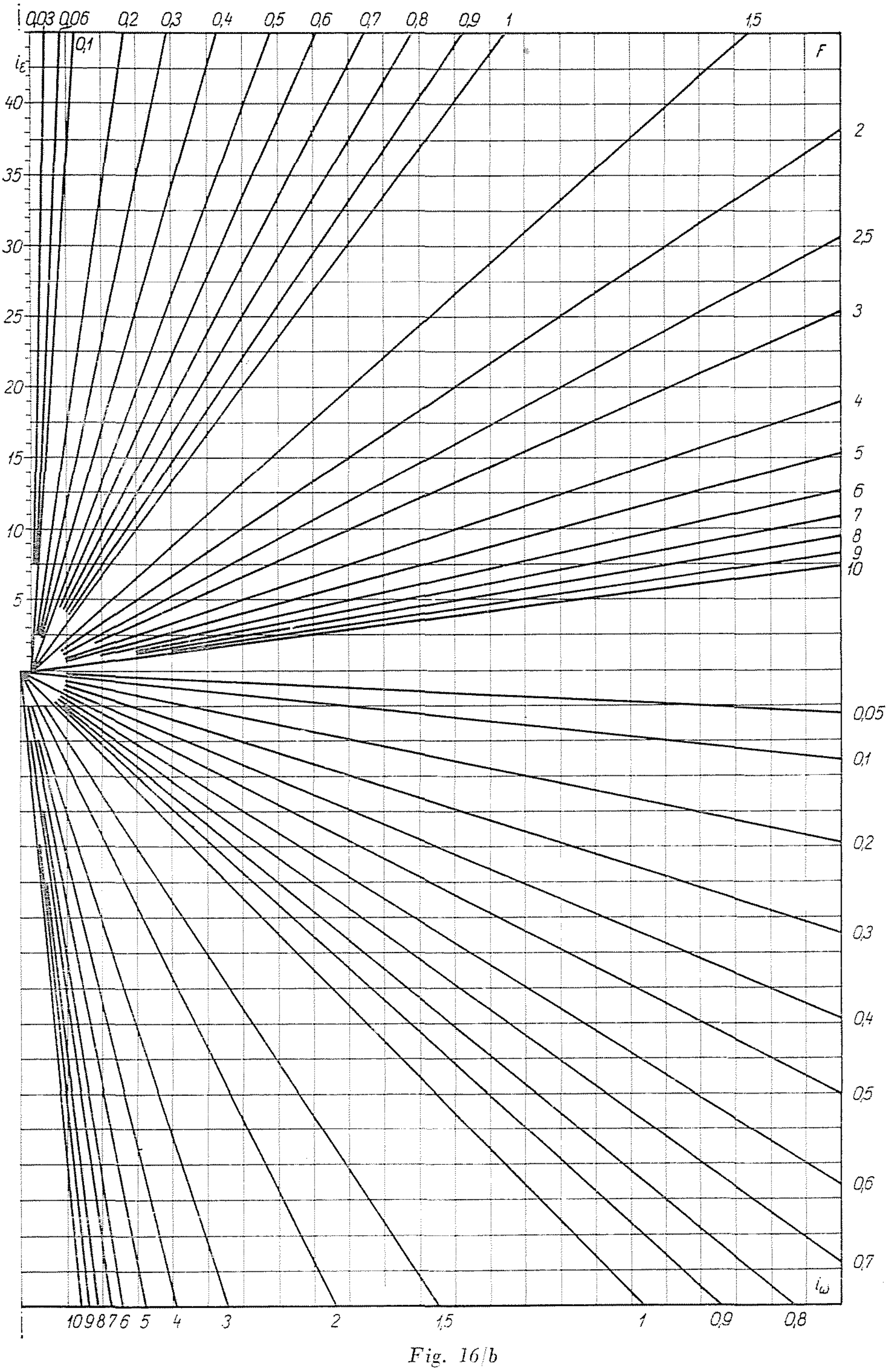

0,03 0,06 0,1 0,2 0,3 0,4 0,5 0,6 0,7 0,8 0,9 1 1,5
F
i_ε
40
35
30
25
20
15
10
5
2
2,5
3
4
5
6
7
8
9
10
0,05
0,1
0,2
0,3
0,4
0,5
0,6
0,7
i_ω
10 9 8 7 6 5 4 3 2 1,5 1 0,9 0,8

Fig. 16/b

Transpose the equation for F:

$$F = -\frac{\sin\beta\,(1-2c\cos\beta+c^2)^2}{2c^2\cos^3\beta+2c\,(1-c^2)\cos^2\beta-(5c^2+c^4)\cos\beta+5c^3-c}\,. \quad (14)$$

The inspection of Equ. (11) proves that there is no such condition under which the angle β^* determining the place of the maximum moment would be independent from F. Namely, this could occur only in case when

$$\frac{-\sin\beta\,(1-2c\cos\beta+c^2)^2}{2\,c^2 F} = 0,$$

yet this expression may be equal to zero only with $\cos\beta > 1$.

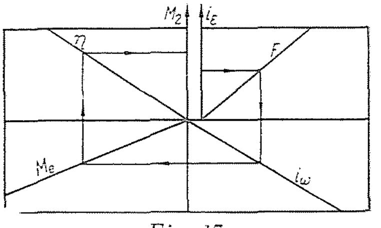

Fig. 17

Fig. 15 demonstrates the set of curves corresponding to Equ. (11). The angle, to which a curve connected to a specified number n comes infinitely close may be computed from the following equation of the third degree:

$$\cos^3\beta^* + \cos\beta^*\,(-0{,}333\;a^2-b) + (0{,}074\;a^3 - 0{,}333\;b\cdot a + d) = 0 \quad (12)$$

where

$$a = \frac{1-c^2}{c}\,;\quad b = \frac{5+c^2}{2}\,;\quad \text{and}\quad d = \frac{5c^2-1}{2c}\,.$$

At a fixed number of slots n the values a, b and c are constant.

For values of F not represented in Fig. 15 the angles β^* may be computed from Equ. (12). Namely, at this portion with a fairly good approximation the angle β^* can be considered independent from F. The smaller the number of slots, the better the approximation.

Thus β^* will be found: for $F < 8$ from Fig. 15, and for $F > 8$ from Equ. (12).

Now i_ω connected to β^* may be determined from Fig. 4. and i_ε from Fig. 6. These values transposed in Equ. (6) give $M_{2_{max}}$. Computation is facilitated by the nomogram given in Fig. 16; for its use see Fig. 17. Like with Fig. 13, also here the magnitudes of the values occurring in the figure may be changed, with the exception of those falling into the first compartment both in Fig. 13 and 16.

Summary

The present paper covers the dynamic analysis of Geneva drives. As a necessary excursus, kinematic conditions had to examined first. Since the questions obtained are difficult to handle, a table and several nomograms were formed to facilitate the determination of kinematic parameters. In the scope of the dynamic analysis a procedure for the determination of the variation in time of the moment acting on the shaft of the Geneva and for the fixing of the number and location of pin reverses has been developed. A method for the determination of the average and maximum moments is presented. Tabulated data and nomograms to facilitate dynamic computations are given. This approach assumes the rigidity of the members of the devices.

References

1. Acserkan, N. Sz.: Fémforgácsoló szerszámgépek számítása és tervezése. Bp., 1953. 606.
2. Артоболевский: Теория механизмов и машин. Москва, 1951.
3. Biezeno, C. B.—Gramell, R.: Technische Dynamic, Berlin, 1939.
4. Ham, C. W.—Crane, E. J.: Mechanics and Machinery, New-York, Toronto, London, McGraw—Hill, Book Company, 1948.
5. Kraemer, O.: Getriebelehre. Karlsruhe, 1950. 189.
6. Lichtwitz, O.: Getriebe für aussetzende Bewegung. Berlin, 1953. 6.
7. Kazinczy, L.: Szerszámgépek I. Budapest, 1955. 313.
8. Smith, M. C.: Geneva Mechanisms, Machine Design, **2**, 163 (1960).
9. Tiplitz, C.: Nomogram gives maximum force acting on Geneva drive rollers. Machine Design, **9**, 127 (1959).
10. Arnesen, L.: Planetary Genewas. Machine Design, **18**, 135 (1959).

E. Filemon, Budapest XI., Sztoczek u. 2. Hungary.